Received: 17 April 2023 | Revised: 6 August 2023 | Accepted: 16 August 2023

DOI: 10.1002/jmor.21636

RESEARCH ARTICLE

JOURNAL OF morphology WILEY

# Predicting body mass in Ruminantia using postcranial measurements

Alexa N. Wimberly

Department of Organismal Biology and Anatomy, University of Chicago, Chicago, Illinois, USA

**Correspondence**
Alexa N. Wimberly
Email: awlamprecht@uchicago.edu

**Funding information**
Smithsonian Institution Pre-Doctoral Fellowship; Field Museum

## Abstract

Size plays an important role in mammalian ecology. Accurate prediction of body mass is therefore critical for inferring aspects of ecology in extinct mammals. The unique digestive physiology of extant ruminant artiodactyls, in particular, is suggested to place constraints on their body mass depending on the type of food resources available. Therefore, reliable body mass estimates could provide insight into the habitat preferences of extinct ruminants. While most regression equations proposed thus far have used craniodental predictors, which for ungulates may produce misleading estimates based on indirect relationships between tooth dimensions and size, postcranial bones support the body and may be more accurate predictors of body mass. Here, I use phylogenetically informed bivariate and multiple regression techniques to establish predictive equations for body mass in 101 species of extant ruminant artiodactyls based on 56 postcranial measurements. Within limb elements, stepwise multiple regression models were typically preferred, though bivariate models often received comparable support based on Akaike's information criterion scores. The globally preferred model for predicting mass is a model including both proximal and distal width of the humerus, though several models from the radioulna received comparable support. In general, widths of long bones were good predictors, while lengths and midshaft circumferences were not. Finally, I show that where the best elements for prediction are unavailable for fossil taxa, selection of the model with lowest percent prediction error for the lowest level clade to which the fossil can be assigned could be a productive and novel way forward for predicting mass and subsequently aspects of ecology in fossil mammals.

**KEYWORDS**
body mass, postcrania, Ruminantia, stepwise multiple regression

## 1 | INTRODUCTION

The ecology, physiology, and morphology of mammalian species all relate, in part, to body mass (Calder, 1996; Damuth & MacFadden, 1990; Eisenberg, 1981; McNab, 1988; Peters, 1986; Schmidt-Nielsen, 1984). Studies at high taxonomic levels have shown relationships between body size and dietary guild membership (e.g., Pineda-Munoz et al., 2016; Price & Hopkins, 2015) and locomotion through foot and limb posture and mechanical efficiency (e.g., Biewener, 1983, 1989; Kubo et al., 2019; Reilly et al., 2007). Body size also relates to other aspects of life history such as home range, where larger mammals often have larger home ranges (Lindstedt et al., 1986; Swihart et al., 1988; Tucker et al., 2014). Therefore, the ability to predict body mass from skeletal proxies is an invaluable tool for inferring the ecology of extinct mammals.

The impressive ecological diversity of living and extinct ruminant artiodactyls (suborder Ruminantia) invites the investigation of reliable skeletal measurements for predicting body mass. Originating around 45 million years ago (Zurano et al., 2019), ruminants exhibit a wide range of body sizes spanning several orders of magnitude, from the under 4 kg chevrotains (or mouse deer, Tragulidae) and small antelopes such as dik-diks (*Madoqua* sp.: Bovidae) to the roughly 1000 kg giraffes (*Giraffa* sp.:Giraffidae). The roughly 230 living species are divided into six families: Tragulidae (chevrotains), Giraffidae (giraffes and okapis), Antilocapridae (pronghorn antelope), Cervidae (deer), Bovidae (cattle, antelope, and kin), and Moschidae (musk deer; Figure 1). Ruminants naturally occur on all continents except for Antarctica and Australia and in doing so, occupy habitats that range from arid deserts through rocky mountain outcrops to tropical rainforests.

Developing body mass estimates for extinct ruminants allows for a more robust understanding of their ecology and evolution. Body mass in fossil mammals is often predicted from craniodental measurements. Dental measurements, particularly the length or area of the first molar, have been widely used as body mass estimators in mammals because they are abundant in fossil assemblages (Alroy, 1998; Damuth & MacFadden, 1990; Gingerich et al., 1982; Legendre, 1986; Legendre & Roth, 1988; Mendoza et al., 2006). However, regression equations based on molar proportions have led to overestimates of body mass in extant carnivorans, where molars are also under selection for dietary specializations (Finarelli & Flynn, 2006; Van Valkenburgh, 1990). In the case of ungulates, and ruminants in particular, differences in food acquisition impact tooth row and cranial dimensions, which biases estimates of body size, necessitating the development of alternative regression equations that are robust to the influences of dietary guild (Janis, 1990).

The postcranial skeleton, particularly limb bones, may provide a more functionally informative estimate of mass due to the role of the limbs as support structures. Long bone lengths have been used in the case of estimating body size in extinct beavers (Reynolds, 2002), but are generally found to be poor predictors, though the length of proximal elements such as the humerus and femur have been proposed as better proxies than the length of distal elements such as metapodials in artiodactyls (Scott, 1983), bovids (Scott, 1985), and ungulates broadly (Scott, 1990). Midshaft circumferences of long bones (particularly the humerus and femur) are widely useful for tetrapods (Anderson et al., 1985; Campione & Evans, 2012) in general, and mammals more specifically (e.g., Anyonge, 1993; Gingerich, 1990; Ruff, 1990), but have the potential to overestimate mass if the species engages in behaviors that exert high stresses on the skeleton, such as digging (Biknevicius, 1999; Millien & Bovy, 2010), because the cross-sectional properties of midshafts are influenced by the force exerted on the bone (Biknevicius, 1993; Ruff, 1990). Additionally, ungulates in general (and especially bovids), show noticeable differences in how their long bone dimensions scale with body mass in comparison to other mammalian groups, particularly in that proximal elements (humerus and femur) are much shorter (Alexander et al., 1979; Bertram & Biewener, 1990; Campione & Evans, 2012; Carrano, 2001; Christiansen, 1999). Understanding the limb postures and locomotor modes in a clade of interest is imperative for identifying reliable predictors of body mass, and therefore requires a reference sample that is numerically large, phylogenetically broad, and biomechanically comparable (Basu

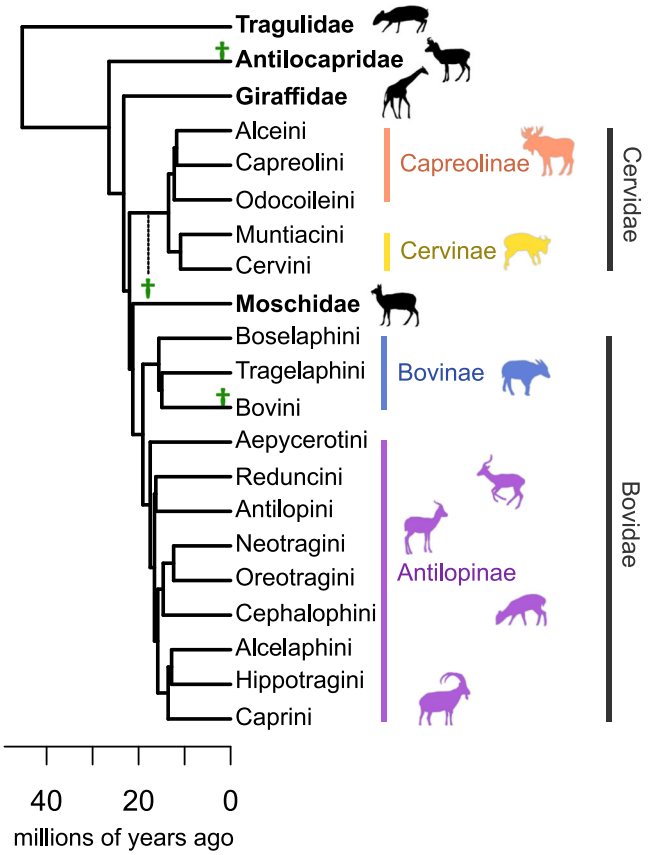


**FIGURE 1** An ultrametric phylogenetic tree visualizing relationships within suborder Ruminantia. Green crosses indicate the placement of fossils used in this study: a fossil antilocaprid (*Cosoryx furcatus*), a fossil bison (*Bison antiquus*), and (*Aletomeryx* sp., part of Cervoidea).

et al., 2016; Bertram & Biewener, 1990; Biewener, 1989, 1990; Ruff, 1990, 2003; Sánchez-Villagra et al., 2003).

Many predictive equations to estimate body mass are generated with the aim of applying them to the fossil record, but taphonomic biases can complicate their application. Long bone elements preserved most frequently in the fossil record are limited to the relatively more robust distal and proximal ends, making prediction of mass from long bone lengths or midshaft measurements less practical. Successful predictors of body mass have also come from proximal and distal ends of long bones, which are expected to correlate with joint loading (Andersson, 2004; Egi, 2001; Kappelman et al., 1997; Ruff, 1988, 1990). Additionally, the robust nature of the astragalus and calcaneus (tarsal bones) allows for increased preservation potential, and these bones have been shown to be valuable predictors of body mass in fossil taxa (Martinez & Sudre, 1995; Tsubamoto, 2014, 2019; Yapuncich et al., 2015). Most body mass predictors are identified by using bivariate regressions, but when a suite of measurements is examined at once, multiple regression can identify the best individual or grouped predictors for a taxonomic group, as long as the sample size is large enough to avoid overfitting with a large number of variables (Damuth & MacFadden, 1990; Figueirido et al., 2011; Mendoza et al., 2006). Exploring the use of multiple regression may offer the ability to examine groups of measurements from proximal and distal ends of long bones and/or the efficacy of using complete tarsal bones to predict mass (Figueirido et al., 2011; Gingerich, 1990; Mendoza et al., 2006; Tsubamoto, 2014).

Here, I use a set of 56 postcranial measurements to estimate body mass in 101 species of suborder Ruminantia, spanning all six extant families, with the intent of capturing a breadth of body masses and phylogenetic relationships. Using phylogenetic generalized least squares (PGLS) models, I first search for accurate bivariate predictors of body mass because finding single measurements may offer the simplest way of predicting mass while dealing with fragmented fossils which may not have all measurements available for a given bone. Then, as more measurement information may increase prediction accuracy, I use stepwise multiple regression models based on individual elements and, in the case of long bones, proximal and distal subsets of measurements as well as suites of measurements related to a single element. Mammalian proximal limb elements exhibit a stronger signal of evolutionary covariation than distal elements (Rothier et al., 2023), which develop later and are more morphologically disparate (Young, 2013), possibly because of the functional demands related to locomotion. I, therefore, expected that proximal measurements would better predict mass in this group. Indeed, I found that the proximal and distal widths of the humerus together best-predicted mass for Ruminantia, but many individual and grouped measurements from the radioulna received comparable support based on Akaike weights. Midshaft circumferences and lengths of long bones were relatively poorer predictors compared to widths of long bones, suggesting that mediolateral widening of limb elements plays an important role in supporting body mass. Finally, I used the single best regression model, as well as models with the lowest percent prediction error (%PE) for specific clades, to estimate body mass for a fossil antilocaprid (*Cosoryx furcatus*), a fossil bison (*Bison antiquus*), and (*Aletomeryx* sp.) which can be considered part of the family Dromomerycidae or Palaeomerycidae (both of which are considered part of Cervoidea).

## 2 | MATERIALS AND METHODS

### 2.1 | Skeletal materials and measurements

I took measurements from specimens of 101 extant species spanning all six extant ruminant families, using collections held in the Field Museum of Natural History (Chicago, IL) and the National Museum of Natural History (Washington, D.C.; Supporting Information: Tables S4-S6). I gathered fossil data from collections at the American Museum of Natural History (New York, NY). I collected a total of 56 measurements from 10 bones: scapula, humerus, radius, ulna, metacarpus, femur, tibia, metatarsus, calcaneus, and astragalus (Figure 2). See supporting information for detailed descriptions of each measurement. I took measurements to 0.01 mm precision using Mitutoyo Digimatic digital calipers or a tape measure to 1 mm precision for bones larger than the maximum caliper size (600 mm). Circumference measurements were made with a flexible measuring tape. My data collection focused only on adult specimens, as indicated by the complete fusion of long bone epiphyses. Wild-collected specimens were preferred, but zoo specimens were used if there was little wild-collected material available for a species. I excluded any domesticated species. To account for potential sexual dimorphism, I aimed to collect data from three male and three female individuals per species when possible. However, I did not use sex as a variable in any of my analyses because it is unlikely that an unassociated limb bone found in the fossil record is able to be attributed to a particular sex. Therefore, species averages were computed for subsequent analyses and for future application to fossil remains.

### 2.2 | Body mass

Body mass data were collected from the literature (Supporting Information: Table S7). I collected multiple body mass averages for each species when available, and used these reported averages to create a species average body mass.

### 2.3 | Phylogeny

All phylogenetic comparative analyses were performed using the maximum clade credibility tree from Zurano et al. (2019). This time-scaled molecular phylogeny is derived from Bayesian inference of topology and branch lengths using mitochondrial genomes for 206 living and recently extinct ruminant species and 21 fossil calibrations.

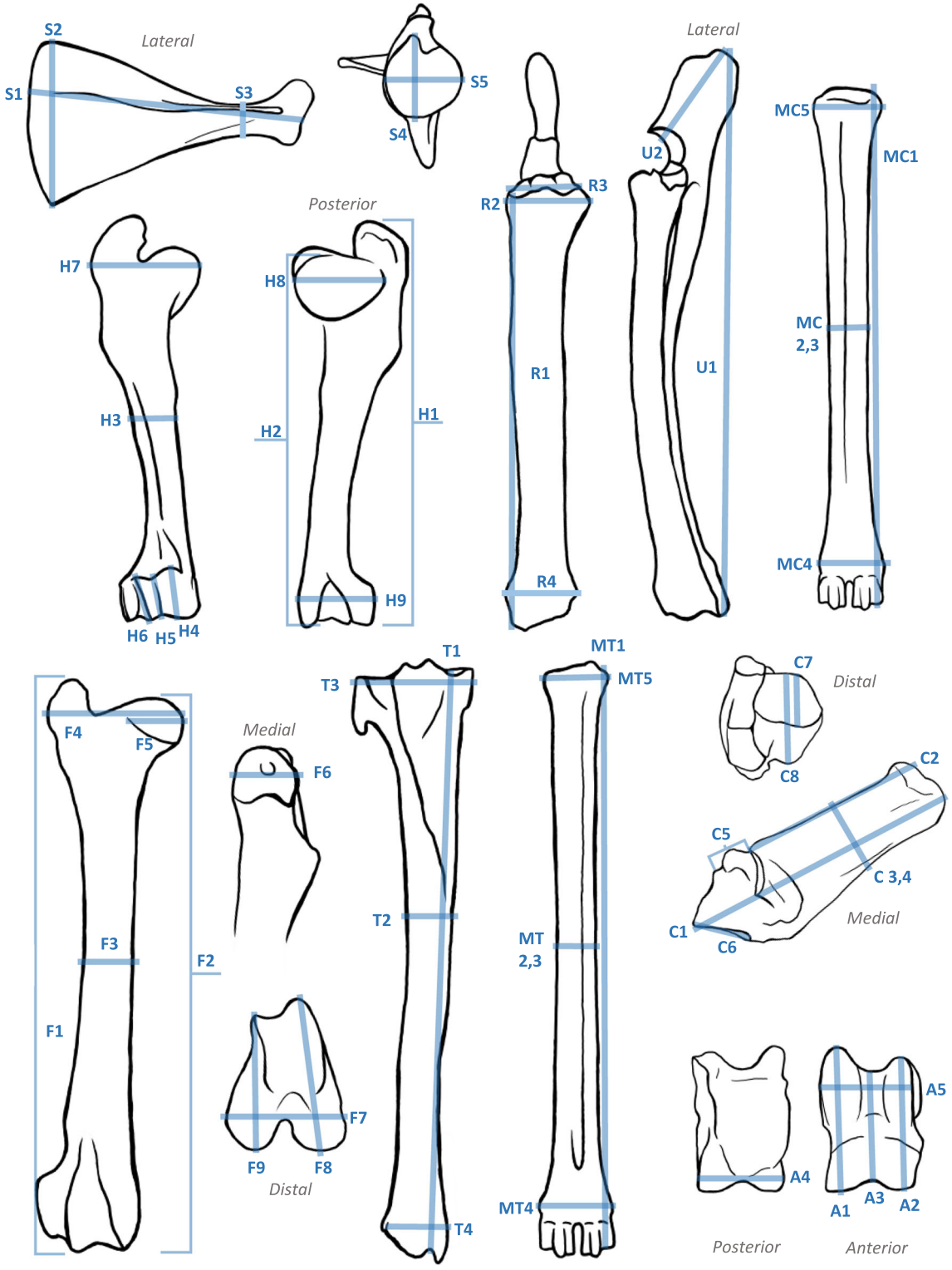


**FIGURE 2** Visualization of the bones used in this study with measurements (lines) and a measurement code. Illustrations are in anterior view unless otherwise noted. Descriptions of each measurement can be found in Supporting Information: Table S3.

## 2.4 | Regressions

### 2.4.1 | Bivariate models

PGLS was performed with the nlme package in R using the function gls() (Pinheiro et al., 2017). PGLS was used to evaluate the relationship between each individual log-transformed measurement and log-transformed average adult body mass (56 total regressions). Pagel's λ was co-estimated using corPagel in the package phytools (Revell, 2012) to assess and account for phylogenetic signal in the residual error term. Bivariate models provide a useful baseline for predicting mass in extinct ruminants due to the potential simplicity of using one effective measurement rather than multiple if that feature is the only part found for a given fossil.

### 2.4.2 | Multiple regression models

Although bivariate regressions are more commonly used to generate predictive equations for estimating body mass, using multiple regressions can increase prediction accuracy (Mendoza et al., 2006). I, therefore, performed stepwise multiple regressions for each postcranial element. I first performed a multiple regression in a phylogenetic framework using the gls() function in the nlme package, as described above. Next, I used stepwise regression to eliminate measurements that did not contribute significantly to predicting mass. To do this, I first refit a multiple regression model using gls() but with lambda fixed to its maximum likelihood estimate and with the method set to "ML" rather than the default option "REML" as stepwise multiple regressions cannot be fit in a restricted maximum likelihood framework and λ cannot be co-optimized under stepwise multiple regression. I then used the step function in the package MASS to run a stepwise multiple regression (Ripley et al., 2013) in both the forward and backward stepwise procedure. Finally, I built a model using the measurements retained by the stepwise regression, which will be referenced as the (given bone) stepwise model. As an alternative way of predicting body mass from multiple measurements while accounting for their covariation, I performed a principal components analysis of the measurements for each element using the function prcomp(). After confirming that all component loadings were of the same magnitude and sign, and that PC1 was, therefore, a "size" axis, I then used the PC1 scores as predictors in a bivariate PGLS model. Complete long bones are infrequently preserved in the fossil record limiting their utility for prediction of body mass in fossil taxa. To account for this taphonomic artifact, I additionally grouped measurements for long bones by proximal and distal ends and repeated the stepwise multiple regression procedure described above.

## 2.5 | Assessing regression models

To assess the relative performance of linear models based on individual measurements, whole elements, and distal/proximal ends of elements for body mass estimation, I used Akaike's information criterion (AIC), as this method prioritizes models that use the fewest parameters (independent variables) while maximizing the variance explained. I used ΔAIC to determine how close an alternative model was to the optimal model (where ΔAIC < 4 is considered a comparable model) and Akaike weights ($AIC_w$) to assess the relative support of each model. I also used AIC to compare how well bivariate and stepwise multiple regressions perform. Information-theoretic approaches can be used to compare regression models with different predictors provided that the sample remains constant across analyses, which it does here. This is because the likelihood of linear regression is a function of the sum of squared residual errors for the response variable, here log body mass, and not the dependent variable(s) used. This logic forms the basis for stepwise regression, which seeks to balance increased likelihoods achieved through incorporation of multiple predictors with a parsimony penalty to avoid the use of additional predictors that yield only minimal decreases in residual error. I use this feature here to assess not only whether single measurements or combinations of multiple measurements from a given bone are more useful for predicting mass in my sample of extant ruminants, but also to determine which elements best predict mass or whether linear combinations of traits might perform better than a simple additive model. I also calculated percent prediction error (%PE) (Smith, 1984; Van Valkenburgh, 1990) in the form of a mean for each regression and for each species, family, subfamily, and tribe (see Supporting Information for results). %PE examines the percent difference between the observed mass and the predicted mass and is obtained using the expression

$$\%PE = \frac{\text{Observed} - \text{Predicted}}{\text{Predicted}} * 100. \quad (1)$$

The merit in using %PE, as opposed to raw residual error, is that it provides a value for each taxon that is easy to interpret and compare across regressions. %PE was calculated from logged species mean body mass values and fitted values from each regression. Counter-intuitively, a negative %PE indicates overprediction, while a positive %PE indicates underprediction.

## 2.6 | Application to fossil ruminants

To assess the efficacy of my regressions developed on extant ruminants, I used them to estimate body mass in select fossil ruminants from North America. These taxa included a specimen of *Bison antiquus* from the late Rancholabrean of New Mexico (Bovidae; AMNH FM 130792), a specimen of *Cosoryx furcatus* from the early Clarendonian of Nebraska (Antilocapridae; AMNH FM 51031), and one specimen of *Aletomeryx* sp. from the Hemingfordian of Nebraska (Cervoidea; AMNH F:AM 42883).

## 3 | RESULTS

### 3.1 | Results by element

All bivariate and multiple regressions were significant ($p < .001$). In most cases, the preferred models for each element, based on AIC, were the stepwise multiple regression models. Exceptions were the metacarpus, metatarsus, and astragalus, for which bivariate regressions were preferred. In most cases, a model based on one measurement received comparable support to the stepwise multiple regression model. All regression equations are presented in Supporting Information (Supporting Information: Table S1). Below, I summarize model fits and performance for each element.

#### 3.1.1 | Scapula

Based on AIC score, the preferred model for predicting body mass using the scapula was the stepwise multiple regression model, which included the greatest craniocaudal length, shortest length of the scapular neck and height of the glenoid fossa (S2 + S3 + S4) (Figure 2). The preferred scapula model also accounted for 85% of the Akaike weights and displayed the lowest residual standard error (0.27; Table 1). The anteroposterior length of the glenoid fossa (S4) was the next most preferred model with a ΔAIC score of 3.46, and accounted for 15% of the model weights. The least preferred model was the greatest cranio-caudal length of the scapula (S2, ΔAIC = 59.86). Although far from best supported (ΔAIC = 11.60), the "all scapula" model, using PC1 scores of all scapular measurements, had the lowest average value of %PE (closest to 0) (Table 1).

#### 3.1.2 | Humerus

The stepwise multiple regression of humerus measurements was the preferred model for predicting mass based on AIC score ($AIC_w$ = 0.91). This model comprises the proximal and distal width measurements (H7 + H9; Table 1). The traditional midshaft circumference measurement of the humerus was a poorer predictor based on AIC values (H3, ΔAIC = 19.85), though assessing model performance using %PE revealed that midshaft circumference had the closest mean %PE to 0 and the smallest range of %PE values. The worst humeral predictors according to AIC scores were the full and functional lengths (H1, ΔAIC = 39.50; H2, ΔAIC = 47.30). Average %PE values for these length measurements of 2.42 and 3.83, respectively, indicate underprediction of mass for species in the sample (Table 1).

#### 3.1.3 | Radius and ulna

The stepwise multiple regression model for the radioulna, made up of the lengths of the radius and ulna with the width of the humeral articular surface at the proximal radius (U1 + R1 + R3), best predicted body mass according to AIC score, though it only accounted for half of the model weights ($AIC_w$ = 0.51). Humeral articular surface width (R3) constituted the best bivariate model for predicting mass (ΔAIC = 1.71, $AIC_w$ = 0.22), followed by the full proximal width (R2, ΔAIC = 2.59, $AIC_w$ = 0.14) and the radius measurements from the stepwise regression (R1 + R3, ΔAIC = 2.98, $AIC_w$ = 0.11; Table 1). Of all postcranial elements, the radioulna had the highest number of models that fell within four AIC units of the optimal model, indicating multiple options for predicting mass from these bones. The model containing the distal width of the radius (R4) had the lowest mean %PE.

#### 3.1.4 | Metacarpus

The best measurement for predicting body mass using the metacarpus was the proximal width (MC5) based on AIC score, which held 50% of the model weights. However, the "best" measurement indicated by stepwise regression was also the proximal width measurement, which explains the other 50% of model weights (Table 1). The length of the metacarpus was the least preferred predictor for mass based on AIC score (ΔAIC = 139.93; Table 1). Metacarpus length also underestimates mass by about 4% based on average %PE, with individual taxa being overestimated by as much as 52% and underestimated by up to 76%.

#### 3.1.5 | Femur

The preferred model for predicting mass using femur measurements based on AIC score was the stepwise multiple regression model. This model included the anteroposterior femoral head measurement and all three distal femur measurements (F6 + F7 + F8 + F9), accounting for a total of 87% of Akaike weights (Table 2). No other models were considered comparable based on ΔAIC scores. Similar to the humerus, the full and functional lengths (F1, ΔAIC = 33.10; F2, ΔAIC = 35.25) were some of the poorest predictors, also including the mediolateral femoral head width (F5, ΔAIC = 31.73) and the midshaft circumference (F3, ΔAIC = 30.66) (Table 2). The distal width of the femur (F7) and functional length (F2) both had close to ideal average %PE values of −0.03 and 0.02, but the distal femur group showed the smallest range of %PE values (Table 2).

#### 3.1.6 | Tibia

Consistent with most other elements, the stepwise multiple regression model was the most preferred for predicting mass, but included all four tibia measurements. Interestingly, this model also showed the smallest range for %PE values out of all models investigated here, with taxa being underestimated by up to about 16% and overestimated by roughly 18% (Table 2). Most Akaike weight was assigned to the stepwise tibia model (76%) though the other

**TABLE 1** Table with model results by forelimb long bone.

| Bone | Model | AIC | ΔAIC | $AIC_w$ | λ | RSE | Mean PPE | Min. PPE | Max. PPE |
|---|---|---|---|---|---|---|---|---|---|
| Scapula | S1 (full length) | 34.02 | 22.28 | 0.00 | 0.70 | 0.28 | 0.34 | −36.02 | 22.60 |
| | S2 (greatest craniocaudal length) | 71.60 | 59.86 | 0.00 | 0.75 | 0.39 | 2.50 | −34.50 | 29.36 |
| | S3 (shortest length of scapular neck) | 33.73 | 21.99 | 0.00 | 0.51 | 0.29 | 2.00 | −30.89 | 20.99 |
| | S4 (anteroposterior glenoid fossa) | 15.20 | 3.46 | 0.15 | 0.75 | 0.29 | −1.73 | −33.06 | 34.74 |
| | S5 (mediolateral glenoid fossa) | 40.10 | 28.35 | 0.00 | 0.84 | 0.34 | −1.70 | −36.88 | 25.94 |
| | All S pca | 23.34 | 11.60 | 0.00 | 0.63 | 0.27 | −0.20 | −32.01 | 21.88 |
| | Scapula stepwise (S2 + S3 + S4) | 11.74 | 0.00 | 0.85 | 0.71 | 0.27 | −0.81 | −30.88 | 32.09 |
| | Glenoid S pca (S4 + S5) | 23.99 | 12.25 | 0.00 | 0.80 | 0.31 | −1.82 | −34.79 | 26.23 |
| Humerus | H1 (full length) | 42.75 | 39.50 | 0.00 | 0.84 | 0.35 | 2.42 | −22.34 | 28.55 |
| | H2 (functional length) | 50.55 | 47.30 | 0.00 | 0.87 | 0.39 | 3.83 | −26.57 | 32.65 |
| | H3 (midshaft circumference) | 23.10 | 19.85 | 0.00 | 0.53 | 0.27 | −0.46 | −22.70 | 27.21 |
| | H4 (largest medial height of trochlea) | 29.90 | 26.65 | 0.00 | 0.89 | 0.33 | −0.73 | −25.51 | 26.27 |
| | H5 (smallest height of trochlea) | 25.39 | 22.14 | 0.00 | 0.89 | 0.34 | −2.50 | −32.66 | 38.63 |
| | H6 (largest lateral height of trochlea) | 25.79 | 22.54 | 0.00 | 0.88 | 0.33 | −1.41 | −26.03 | 30.11 |
| | H7 (proximal width) | 10.21 | 6.96 | 0.03 | 0.77 | 0.32 | −3.72 | −32.92 | 61.02 |
| | H8 (mediolateral humeral head width) | 19.02 | 15.77 | 0.00 | 0.78 | 0.29 | −1.26 | −23.66 | 26.76 |
| | H9 (distal width) | 17.86 | 14.61 | 0.00 | 0.72 | 0.32 | 4.02 | −29.48 | 26.26 |
| | All H pca | 11.99 | 8.74 | 0.01 | 0.76 | 0.27 | −0.58 | −21.57 | 30.59 |
| | Humerus stepwise (H7 + H9) | 3.25 | 0.00 | 0.91 | 0.69 | 0.25 | −0.96 | −22.83 | 33.40 |
| | Prox H pca (H7 + H8) | 9.27 | 6.02 | 0.04 | 0.76 | 0.29 | −2.65 | −28.18 | 43.13 |
| | Dist H pca (H4 + H5 + H6 + H9) | 18.46 | 15.21 | 0.00 | 0.84 | 0.29 | −0.54 | −23.22 | 26.36 |
| Radioulna | U1 (ulna length) | 67.10 | 62.69 | 0.00 | 0.94 | 0.45 | 0.46 | −35.04 | 35.60 |
| | U2 (olecranon process length) | 40.48 | 36.07 | 0.00 | 0.74 | 0.34 | −2.97 | −27.16 | 32.21 |
| | R1 (radius length) | 83.84 | 79.43 | 0.00 | 0.97 | 0.53 | 2.15 | −37.88 | 40.61 |
| | R2 (full proximal width) | 7.00 | 2.59 | 0.14 | 0.76 | 0.29 | −1.96 | −25.13 | 52.59 |
| | R3 (width of humeral articular surface) | 6.12 | 1.71 | 0.22 | 0.69 | 0.27 | −1.45 | −22.76 | 43.11 |
| | R4 (distal width) | 15.27 | 10.87 | 0.00 | 0.71 | 0.28 | −0.37 | −19.15 | 31.36 |
| | All RU pca | 26.73 | 22.32 | 0.00 | 0.83 | 0.32 | −1.14 | −27.04 | 41.92 |
| | RU stepwise (U1 + R1 + R3) | 4.41 | 0.00 | 0.51 | 0.59 | 0.26 | −2.03 | −21.13 | 40.62 |
| | Radius stepwise (R1 + R3) | 7.39 | 2.98 | 0.11 | 0.61 | 0.26 | −1.59 | −21.21 | 41.49 |
| | Ulna stepwise (U1 + U2) | 38.29 | 33.88 | 0.00 | 0.77 | 0.33 | −2.41 | −28.44 | 35.87 |
| | All R pca (R1 − R4) | 22.21 | 17.80 | 0.00 | 0.83 | 0.31 | −0.80 | −25.52 | 43.30 |
| | All U pca (U1 + U2) | 42.05 | 37.64 | 0.00 | 0.85 | 0.35 | −1.63 | −30.39 | 37.07 |
| | Prox RU pca (U2 + R2 + R3) | 10.44 | 6.04 | 0.02 | 0.67 | 0.28 | −2.26 | −24.38 | 44.35 |
| Metacarpus | MC1 (length) | 157.67 | 139.93 | 0.00 | 1.01 | 0.88 | 4.01 | −52.34 | 76.67 |
| | MC2 (anteroposterior midshaft) | 74.04 | 56.31 | 0.00 | 0.91 | 0.42 | −2.50 | −36.58 | 66.31 |
| | MC3 (mediolateral midshaft) | 67.63 | 49.90 | 0.00 | 0.76 | 0.37 | 2.17 | −28.08 | 27.68 |
| | MC4 (distal width) | 38.10 | 20.37 | 0.00 | 0.74 | 0.32 | 1.21 | −22.47 | 26.57 |
| | MC5 (proximal width) | 17.73 | 0.00 | 0.50 | 0.75 | 0.30 | −1.69 | −23.35 | 49.35 |

(Continues)

**TABLE 1** (Continued)

| Bone | Model | AIC | ΔAIC | $AIC_w$ | λ | RSE | Mean PPE | Min. PPE | Max. PPE |
|---|---|---|---|---|---|---|---|---|---|
| | All MC pca | 47.11 | 29.38 | 0.00 | 0.86 | 0.36 | −1.12 | −29.40 | 42.39 |
| | MC stepwise (MC5) | 17.73 | 0.00 | 0.50 | 0.75 | 0.30 | −1.69 | −23.35 | 49.35 |

*Note*: AIC score, AIC weight, RSE, lambda, mean %PE, minimum and maximum %PE. All %PE values are log-transformed. Organized by bone.
Abbreviations: AIC, Akaike's information criterion; MC, metacarpus; pca, principal components analysis; PPE, percent prediction error; RSE, residual standard error; RU, radioulna.

**TABLE 2** Table with model results by hindlimb long bone.

| Bone | Model | AIC | ΔAIC | $AIC_w$ | λ | RSE | Mean PPE | Min. PPE | Max. PPE |
|---|---|---|---|---|---|---|---|---|---|
| Femur | F1 (full length) | 40.89 | 33.10 | 0.00 | 0.87 | 0.33 | −0.52 | −23.11 | 27.17 |
| | F2 (functional length) | 43.04 | 35.25 | 0.00 | 0.88 | 0.34 | 0.02 | −22.93 | 27.76 |
| | F3 (midshaft circumference) | 38.45 | 30.66 | 0.00 | 0.71 | 0.30 | 1.39 | −28.03 | 25.91 |
| | F4 (proximal width) | 14.11 | 6.32 | 0.04 | 0.80 | 0.29 | −0.99 | −24.69 | 18.31 |
| | F5 (mediolateral femoral head) | 39.53 | 31.73 | 0.00 | 0.80 | 0.32 | −1.79 | −23.03 | 23.04 |
| | F6 (anteroposterior femoral head) | 16.42 | 8.62 | 0.01 | 0.64 | 0.26 | −1.49 | −27.60 | 31.90 |
| | F7 (distal width) | 13.70 | 5.91 | 0.05 | 0.73 | 0.26 | −0.03 | −22.15 | 18.99 |
| | F8 (medial condyle and patellar lip) | 20.84 | 13.04 | 0.00 | 0.89 | 0.33 | 1.70 | −25.19 | 25.64 |
| | F9 (lateral condyle and patellar lip) | 22.82 | 15.02 | 0.00 | 0.86 | 0.30 | 0.52 | −19.82 | 25.70 |
| | All F pca | 17.06 | 9.27 | 0.01 | 0.76 | 0.27 | −0.48 | −21.33 | 19.54 |
| | Femur stepwise (F6 + F7 + F8 + F9) | 7.80 | 0.00 | 0.87 | 0.71 | 0.26 | −0.21 | −22.39 | 22.23 |
| | Prox F pca (F4 + F5 + F6) | 17.21 | 9.41 | 0.01 | 0.71 | 0.27 | −1.61 | −24.59 | 23.07 |
| | Dist F pca (F7 + F8 + F9) | 16.24 | 8.45 | 0.01 | 0.83 | 0.29 | 0.62 | −18.81 | 21.98 |
| Tibia | T1 (full length) | 94.82 | 86.03 | 0.00 | 0.97 | 0.51 | −0.83 | −37.73 | 42.68 |
| | T2 (midshaft circumference) | 46.23 | 37.44 | 0.00 | 0.79 | 0.33 | 0.91 | −31.18 | 24.02 |
| | T3 (proximal width) | 11.23 | 2.44 | 0.23 | 0.74 | 0.26 | −0.36 | −21.17 | 21.83 |
| | T4 (distal width) | 17.02 | 8.23 | 0.01 | 0.80 | 0.29 | 1.08 | −20.48 | 19.09 |
| | All T pca | 35.78 | 26.99 | 0.00 | 0.86 | 0.32 | −0.28 | −27.90 | 26.06 |
| | Tibia stepwise (T1 + T2 + T3 + T4) | 8.79 | 0.00 | 0.76 | 0.72 | 0.26 | 0.34 | −16.20 | 18.24 |
| Metatarsus | MT1 (length) | 152.96 | 127.95 | 0.00 | 1.01 | 0.88 | 6.79 | −46.56 | 89.66 |
| | MT2 (anteroposterior midshaft) | 77.22 | 52.21 | 0.00 | 0.95 | 0.46 | −2.14 | −36.51 | 27.37 |
| | MT3 (mediolateral midshaft) | 58.62 | 33.61 | 0.00 | 0.74 | 0.36 | 2.49 | −24.63 | 28.11 |
| | MT4 (distal width) | 46.91 | 21.90 | 0.00 | 0.67 | 0.35 | 3.09 | −26.38 | 25.09 |
| | MT5 (proximal width) | 25.01 | 0.00 | 0.55 | 0.80 | 0.30 | −0.68 | −24.70 | 22.79 |
| | All MT pca | 55.28 | 30.27 | 0.00 | 0.89 | 0.39 | 0.54 | −28.22 | 27.77 |
| | MT stepwise (MT1 + MT5) | 25.40 | 0.39 | 0.45 | 0.72 | 0.28 | −0.78 | −22.89 | 21.20 |

*Note*: AIC score, AIC weight, RSE, lambda, mean %PE, minimum and maximum %PE. All %PE values are log-transformed.
Abbreviations: AIC, Akaike's information criterion; MT, metatarsus; pca, principal components analysis; PPE, percent prediction error; RSE, residual standard error.

significant proportion of weight was assigned to the proximal width (T3, 23%), which also fell within four AIC units of the optimal model (Table 2). Tibia length (T1) was considered the least preferred model for predicting mass (ΔAIC = 86.03).

### 3.1.7 | Metatarsus

Similar to the metacarpus, the proximal width of the metatarsus (MT5) was the best measurement for predicting body mass based on

AIC score for this element ($AIC_w$ = 0.55). However, the stepwise multiple regression model indicated that the proximal width in combination with the full length of the metatarsus was a comparably effective model (MT1 + MT5; ΔAIC = 0.39, $AIC_w$ = 0.45) (Table 2). The least preferred model based on AIC scores was the full length of the metatarsus alone (MT1, ΔAIC = 127.95). The range of %PE values for metatarsus length is also wide, with overestimations up to roughly 47% and underestimations reaching about 90%.

#### 3.1.8 | Calcaneus

Based on AIC score, the best model for predicting body mass using the calcaneus was the stepwise multiple regression calcaneus model ($AIC_w$ = 0.85). This model included midbody height (C3), cubonavicular facet length (C6), height of the sustentacular facet (C7), and the height of the sustentaculum tali (C8) (Table 3). The last measurement, height of the sustentaculum tali, was the most preferred individual measurement and fell just within four AIC units of the optimal model (ΔAIC = 3.54).

#### 3.1.9 | Astragalus

Like most other elements, the stepwise multiple regression model was the optimal model for predicting mass from the astragalus, but it consisted of only one measurement, the width at the tarsus (A4). This model and its univariate counterpart combined accounted for 98% of model weight (Table 3).

### 3.2 | All models compared

The best model, out of 84 considered, was the stepwise multiple regression model from the whole humerus (H7 + H9; $AIC_w$ = 0.36; Supporting Information: Table S1). Models that fell within four AIC units of the optimal model were the stepwise multiple regression based on radioulna measurements (U1 + R1 + R3; ΔAIC = 1.16; $AIC_w$ = 0.2), stepwise multiple regression based on calcaneus measurements (C3 + C6 + C7 + C8; ΔAIC = 2.24; $AIC_w$ = 0.12), R3 (ΔAIC = 2.87; $AIC_w$ = 0.08), and R2 (ΔAIC = 3.75; $AIC_w$ = 0.05; Supporting Information: Table S1). The three worst predictors were the length of the tibia (T1, ΔAIC = 91.57), length of the metatarsus (MT1, ΔAIC = 149.71), and length of the metacarpus (MC1, ΔAIC = 154.42).

Plotting predicted ruminant body mass based on the stepwise humerus regression against observed values shows little deviation from an ideal prediction represented by the gray 1-1 line in Figure 3 (left). Mean %PE over the entire suborder for this regression is −0.96 (Table 1), but is much more variable at lower levels. The humerus stepwise multiple regression overestimates body mass for Antilocapridae (%PE = −7.73), Giraffidae (%PE = −3.46), and Moschidae

**TABLE 3** Table with model results by tarsal bone.

| Bone | Model | AIC | ΔAIC | $AIC_w$ | λ | RSE | Mean PPE | Min. PPE | Max. PPE |
|---|---|---|---|---|---|---|---|---|---|
| Calcaneus | C1 (greatest length) | 36.37 | 30.88 | 0.00 | 0.83 | 0.33 | 0.55 | −22.76 | 25.42 |
| | C2 (length of body) | 48.10 | 42.61 | 0.00 | 0.89 | 0.36 | −0.63 | −25.98 | 27.93 |
| | C3 (midbody height) | 37.00 | 31.51 | 0.00 | 0.85 | 0.33 | 1.18 | −28.42 | 29.45 |
| | C4 (midbody transverse width) | 69.37 | 63.88 | 0.00 | 0.90 | 0.47 | 6.01 | −42.17 | 38.57 |
| | C5 (fibular facet length) | 66.98 | 61.49 | 0.00 | 0.87 | 0.41 | −3.02 | −38.24 | 90.55 |
| | C6 (cubonavicular facet length) | 76.02 | 70.53 | 0.00 | 0.90 | 0.39 | 0.69 | −35.21 | 53.31 |
| | C7 (height of sustentacular facet) | 31.50 | 26.01 | 0.00 | 0.70 | 0.31 | 3.03 | −31.39 | 25.17 |
| | C8 (height of sustentaculum tali) | 9.03 | 3.54 | 0.15 | 0.62 | 0.24 | −0.61 | −22.65 | 45.06 |
| | All C pca | 28.61 | 23.12 | 0.00 | 0.82 | 0.29 | 0.13 | −24.09 | 21.58 |
| | Calcaneus stepwise (C3 + C6 + C7 + C8) | 5.49 | 0.00 | 0.85 | 0.50 | 0.23 | 0.42 | −14.71 | 20.38 |
| Astragalus | A1 (maximum lateral length) | 32.60 | 13.26 | 0.00 | 0.78 | 0.30 | 0.13 | −23.29 | 40.13 |
| | A2 (maximum medial length) | 32.99 | 13.66 | 0.00 | 0.77 | 0.30 | −0.89 | −28.09 | 54.79 |
| | A3 (minimal length) | 38.55 | 19.22 | 0.00 | 0.77 | 0.30 | −0.31 | −29.14 | 48.97 |
| | A4 (width at tarsus) | 19.33 | 0.00 | 0.49 | 0.72 | 0.27 | −0.75 | −22.39 | 35.78 |
| | A5 (width at trochlea) | 26.25 | 6.91 | 0.02 | 0.78 | 0.30 | 0.68 | −21.35 | 21.29 |
| | All A pca | 27.72 | 8.39 | 0.01 | 0.75 | 0.28 | −0.35 | −23.07 | 42.94 |
| | Astragalus stepwise (A4) | 19.33 | 0.00 | 0.49 | 0.72 | 0.27 | −0.75 | −22.39 | 35.78 |

*Note*: AIC score, AIC weight, RSE, lambda, mean %PE, minimum and maximum %PE. All %PE values are log-transformed.

Abbreviations: AIC, Akaike's information criterion; pca, principal components analysis; PPE, percent prediction error; RSE, residual standard error.

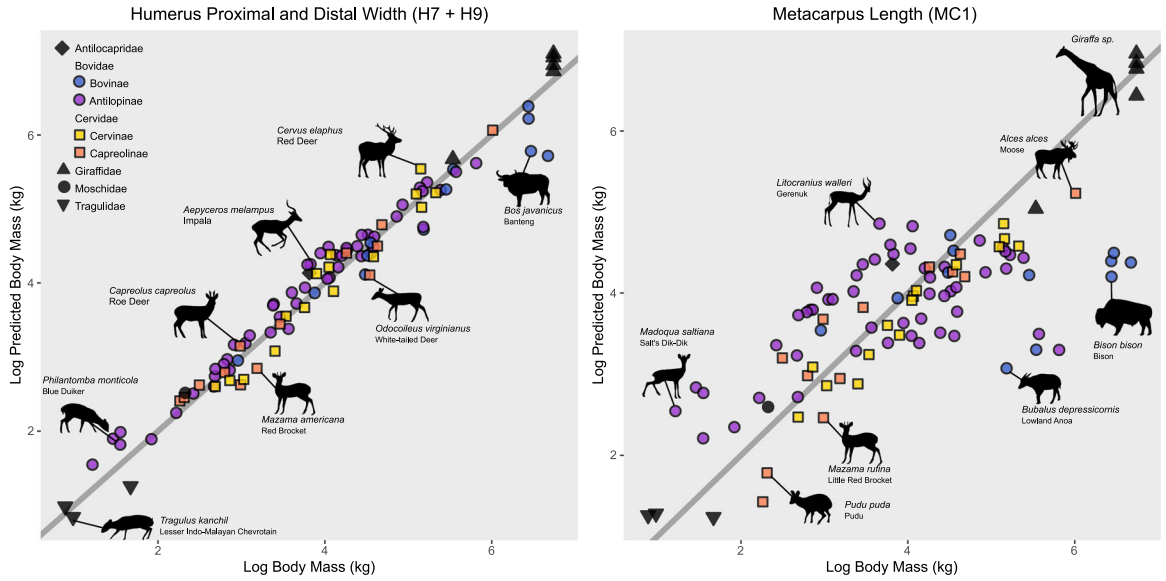


**FIGURE 3** Compared plots of the most preferred model for predicting mass (humerus proximal and distal width combined, left) and least preferred model for predicting mass (metacarpus length, right) based on AIC score on element-specific regressions. Log species-averaged body mass (x) is plotted against log predicted body mass (y). A perfect prediction is indicated by the gray one-toone line. Species falling above the line are overpredicted, while species falling below the line are underpredicted. Silhouettes are provided by PhyloPic or created by the author.

(%PE = −7.59) but underpredicts for Tragulidae (%PE = 13.94; Table 4). Cervidae has a mean %PE of 1.26, but at the tribe level Capreolini body mass is overestimated by about 5% and Muntiacini is underestimated by about 8%. Bovidae has an average %PE of −2.25, but body mass within bovid tribes can be underpredicted by as much as 7% (Bovini) and overpredicted by almost 10% (Aepycerotini; Table 4). The worst regression model based on AIC scores, the MC1 regression, underpredicts ruminant mass on average (%PE = 4.01), but subclade level differences are even more extreme than for the stepwise humerus model. For example, the mean %PE for Bovidae is −2.55 based on metacarpus length, with subfamily Antilopinae overestimated by nearly 3% and subfamily Bovinae underestimated on average by almost 30% (Table 4). The tribes Antilopini and Bovini display the extremes for the range of %PE for metacarpus length of −24.33 and 56.25, respectively. Differences in %PE at the subclade level are clearly shown in Figure 3 (right), where Bovini and large members of Caprini are severely underpredicted, as are most members of Cervidae. Antilopinae are variable, but tribe Antilopini are consistently found above the gray 1-1 line, indicating overestimation.

While the differing %PE values are an extreme case in the example of metacarpus length, even with the globally preferred regression of humerus measurements, there exists clade-level variation that should not be ignored. Differences in %PE at the subclade level may inform model choice for body size estimation of fossil materials, particularly when the overall best humeral model cannot be used due to incomplete remains. Determining the lowest level of classification possible for a fossil and which model here has the closest %PE value to 0 for that taxonomic level can inform which regression to use for body size estimation (see supplement for species-level %PE scores by model as well as Supporting Information: Table S2 which shows what model has the lowest %PE for each family, subfamily, and tribe).

## 3.3 | Fossil estimations

In light of the finding that %PE identifies different optimal models for subclades than are identified by global AIC comparisons, I estimated the body mass of the three fossil taxa using different regression equations and compared the resulting predictions. Because the humerus stepwise multiple regression was considered the global optimal model for all ruminants, I first used that regression. I found those predictions to be as follows: *C. furcatus* (AMNH FM 51031) as 14.64 kg, *Aletomeryx* sp. (AMNH F:AM 42883) as 22.16 kg, and *B. antiquus* (AMNH FM 130792) as 800.45 kg (Table 5).

I then applied the appropriate regression based on a mean %PE closest to 0 for the lowest-level clade to which each fossil taxon could be assigned to assess how well a chosen model based on %PE performs relative to the global best estimate. *Cosoryx furcatus* (AMNH FM 51031) is a member of the subfamily Merycodontinae within Antilocapridae, which has one remaining species (pronghorn antelope *Antilocapra americana*). I, therefore, used the lowest %PE model for *Antilocapra americana* (T2, tibia midshaft circumference) to estimate a body mass of 14.05 kg for this specimen, which is only 4% less than the estimate derived from global best humerus model (Table 5). The closest extant taxonomic level to *Aletomeryx* sp. is likely Cervidae, because *Aletomeryx* belongs to the subfamily Aletomerycinae, which is considered to be part of the family Dromomerycidae or can be grouped with the European palaeomerycids in the family

**TABLE 4** PPE for each family, subfamily, and tribe for the most preferred model (humerus proximal and distal widths) and the least preferred model, length of the metacarpus (MC1).

| Family | Subfamily | Tribe | H7 + H9 | MC1 |
|---|---|---|---|---|
| Antilocapridae | | | −7.73 | −11.86 |
| Bovidae | | | −2.25 | 3.56 |
| | Antilopinae | | −3.92 | −2.55 |
| | | Aepycerotini | −9.98 | −13.94 |
| | | Alcelaphini | −2.44 | 9.51 |
| | | Antilopini | −5.80 | −24.33 |
| | | Caprini | −3.10 | 24.91 |
| | | Cephalophini | −4.45 | −11.35 |
| | | Hippotragini | 1.78 | 17.00 |
| | | Neotragini | 1.82 | −18.41 |
| | | Oreotragini | −2.09 | −1.36 |
| | | Reduncini | −5.54 | −0.61 |
| | Bovinae | | 4.87 | 29.51 |
| | | Boselaphini | 0.13 | −16.17 |
| | | Bovini | 7.05 | 56.25 |
| | | Tragelaphini | 3.20 | 6.56 |
| Cervidae | | | 1.26 | 7.58 |
| | Capreolinae | | 0.91 | 7.47 |
| | | Alceini | −0.98 | 15.92 |
| | | Capreolini | −5.02 | −20.17 |
| | | Odocoileini | 2.28 | 12.15 |
| | Cervinae | | 1.58 | 7.67 |
| | | Cervini | −0.81 | 6.34 |
| | | Muntiacini | 8.13 | 6.25 |
| Giraffidae | | | −3.46 | 2.95 |
| Moschidae | | | −7.59 | −10.49 |
| Tragulidae | | | 13.94 | −7.90 |

*Note*: %PE values are log-transformed.

Abbreviation: PPE, percent prediction errors.

Palaeomerycidae, though both families are considered to be part of Cervoidea (Janis & Scott, 1987; Janis & Theodor, 2014; Prothero & Liter, 2008). Using the preferred model for Cervidae (the radius stepwise model), I estimated *Aletomeryx* to be 23.21 kg (nearly 5% more than the global best estimate; Table 5). *Bison antiquus* can be assigned to the extant tribe Bovini. Using the Bovini-level regression based on %PE closest to 0 (humerus proximal width), I estimated this particular specimen of *B. antiquus* to be 883.89 kg, an increase of about 10% from the estimate based on both the humerus proximal and distal widths (Table 5).

## 4 | DISCUSSION

A taxonomically broad and biomechanically comparable sample of extant mammals is essential for generating accurate predictors of body mass in fossil mammals. Measurements throughout the postcranial skeleton examined individually and in groups by bone and by long bone region, show that long bone lengths are poor predictors of body mass in ruminants, as previously found in bovids and other ungulates (Scott, 1983, 1985, 1990). Previous research also found that long bone midshaft circumferences were good predictors of body mass, but here, these measurements showed weaker relationships with body mass in ruminants than other measurements. Widths of long bones were more informative, which suggests that alterations to limb elements in response to changes in mass happens primarily with transverse widening of long bones (Scott, 1985), and the best predictors of body mass in ruminants are found in using the humerus and radioulna. Groups of multiple measurements, as determined by stepwise regression, are usually found to be better predictors of mass though individual measurements are usually comparable for a given bone. Understanding which regressions are more preferred at different taxonomic levels can generate more informed predictions of body mass in extinct taxa.

### 4.1 | Inferences from long bone lengths and circumferences

The uniqueness of the ruminant postcranial skeleton relative to other mammals is well recognized (Alexander et al., 1979; Bertram & Biewener, 1990; Campione & Evans, 2012; Carrano, 2001; Christiansen, 1999). Indeed, postural changes to the limb in ruminants may account for the difference in my results on long bone length and midshaft measurements compared to previous studies performed on mammal- and tetrapod-wide samples. The shift from crouched postures to more upright and columnar limbs found in ungulates generally are suggested to be related to increases in body size relative to other mammals (Kubo et al., 2019) and increase the effective mechanical advantage of the limb, allowing species with upright limbs to mitigate stresses on the limb during locomotion (Bertram & Biewener, 1990; Biewener, 1983, 1989, 1990; Reilly et al., 2007). Differences in limb posture, therefore, present a fundamental difference in how unguligrade mammals handle stress in their appendicular skeleton and how this may uniquely affect which features best predict body mass in Ruminantia.

Long bones have been widely used for body mass estimation because of their role as support structures (Anyonge, 1993; Damuth & MacFadden, 1990; Egi, 2001; Gingerich, 1990; Reynolds, 2002; Scott, 1983, 1985, 1990). While some studies have found the lengths of the humerus and femur to be reliable predictors of body mass in mammals (e.g., Gingerich, 1990; Reynolds, 2002) and others have found the lengths of these proximal elements to be relatively better predictors than lengths of distal bones (tibia, metapodials, etc. Damuth & MacFadden, 1990; Scott, 1983, 1985, 1990), my results,

**TABLE 5** Estimations for fossil specimens based on clade-specific regressions: the global best estimate (H7 + H9) for all ruminants, tibia midshaft circumference (T3) for Antilocapridae (applied to *Cosoryx furcatus*), the stepwise multiple regression of the radius (R1 + R3) for Cervidae (applied to *Aletomeryx*), and the proximal width of the humerus (H7) for Bovini (applied to *Bison antiquus*).

| Specimen | Family | Global best Estimate | Clade-specific Estimate |
|---|---|---|---|
| *Cosoryx furcatus* AMNH FM 51031 | Antilocapridae | 14.64 | 14.05 |
| *Aletomeryx* sp. AMNH F:AM 42883 | Cervoidea | 22.16 | 23.21 |
| *Bison antiquus* AMNH FM 130792 | Bovidae | 800.45 | 883.89 |

which consider the dimensions of all appendicular elements, indicate that long bone lengths are some of the worst predictors of mass regardless of which bone is being considered and whether full length or functional length is used, as is the case for the humerus and femur. The femur is usually relatively shorter in ungulates than in other mammals (Carrano, 2001); in cursorial species, the stylopodial elements (humerus and femur) shorten relative to more distal elements, which is associated with a proximal concentration of muscle mass on the limb and lighter, more elastically energized distal limbs for increased stride length. This relationship between distal limb lengthening and proximal limb shortening is commonly used as an "index of cursoriality" through the metatarsal/femur ratio to assess limb proportions relative to running ability (e.g., Bakker, 1983; Gambaryan, 1974; Garland & Janis, 1993; Howell, 1944; Janis & Wilhelm, 1993; Smith & Savage, 1956), and may explain why stylopodial element lengths perform more poorly as mass estimators in ruminants than in other clades. Similarly, while midshaft measurements have been equally popular in the literature for predicting mass among a variety of tetrapod groups because long bone midshafts provide cylindrical support for load-bearing in the limb (Anderson et al., 1985; Campione & Evans, 2012; Ruff, 1990), midshaft circumferences did not perform well in my study. Midshaft circumference measurements for this study were taken from the humerus, femur, and tibia, but excluded for the radius because it is fused with the ulna in varying degrees along the midshaft, thus obscuring an appropriate circumference measurement. Taken together, the differences in length and midshaft circumferences of the humerus and femur in ruminants (and ungulates) due to postural differences relative to other mammals and tetrapods explain why these measurements may not be as effective for predicting body mass in this group.

The use of long bone lengths in fossil ruminant ecology may alternatively be found in reconstructing relationships with habitat, as Scott (1983, 1985) suggested that distal limb proportions, in particular, may adapt more quickly to changes in substrate than mass. For example, metacarpus length (MC1) was the least preferred model for predicting mass relative to all other bivariate and multiple regressions, though when %PE is plotted, patterns relating to phylogeny and possibly functional and ecological differences seem to show (Figure 3, right). For example, body mass for the Bovini is severely underpredicted based on metacarpus length (average %PE = 56.25). Two large members of the tribe Caprini (the muskox [*Ovibos moschatus*] and takin [*Budorcas taxicolor*]) are also well underpredicted using metacarpus length. Large caprines and members of Bovini have characteristically short and blocky metacarpals compared to other ruminants, which may be an artifact of their large body size or functional demands of living in rocky/mountainous terrains (as is for the case in the caprines) and suggests a deviation from how other ungulate metacarpals (like those of giraffes) scale with extremely large sizes. At the other extreme, body mass of the ruminants in tribe Antilopini are consistently overpredicted by metacarpus length with an average %PE of roughly −24%, as they have long, gracile extremities and tend to occur in open habitats (Table 4, Figure 3). These patterns provide an interesting platform on which to explore the functional associations between habitat and body mass in ungulates in the future, particularly through a developmental lens where proximal limb segments are more constrained in morphology relative to distal limb elements which may reflect functional variation related to locomotion and habitat (Rothier et al., 2023; Scott, 1985; Young, 2013).

## 4.2 | Long bone widths and body mass

Noticeable changes in length and diameter suggest that long bones become overall more robust in larger mammalian species (Bertram & Biewener, 1990, 1992), particularly in mammals above 300 kg (Biewener, 1990). Robustness, in this study, is captured by midshaft circumference and length, but mediolateral widths may be an important factor in determining how robustness plays a role in strengthening bone to withstand changes in mass. Scott (1985) suggested that, in bovid metapodials, the width increases at a faster rate with increasing body mass at distal ends compared to proximal ends, and that anteroposterior diameters did not significantly change with mass. While this project did not specifically test scaling patterns of metacarpal/metatarsal shape with body mass, I did find that the proximal ends of these bones displayed the highest correlation with mass of all metacarpal and metatarsal measurements (Table 1, Table 2). A personal communication from McMahon (T.M.) in Scott (1985) stated that widening articular surfaces of metapodials for stabilization resulted in a widening of metapodial proximal and distal widths, and Scott (1985) proposed that turning while running might induce lateral forces on the limbs. Both stabilization and lateral forces during turns may induce transverse stresses acting on the

appendicular skeleton, which suggests a connection between bone widths and body mass.

Proximal width measurements alone were considered an optimal model for predicting mass from the radius (R2, R3), metacarpus (MC5), tibia (T3), and metatarsus (MT5), and both the proximal and distal widths of the humerus were the optimal model for predicting mass from the humerus (H7 + H9). It can be inferred then that widths are the most informative measurements, regardless of the element in question. Interestingly, the width of the humeral articular surface of the radius (R3) and the full proximal width of the radius including the lateral tuberosity (R2) were similarly preferred for predicting mass from radioulna measurements, indicating that widths regardless of association to facet shape or whole width are useful for predicting mass in Ruminantia.

### 4.3 | Predicting from the radioulna

Width measurements of the humerus were considered the most preferred model for predicting mass in ruminant artiodactyls, but radioulna models occurred more frequently among the set of top models than did models derived from any other element, and were similarly preferred to the globally preferred humerus model based on AIC scores. A diagnostic feature of ungulate cursors is the fusion of the radius and ulna, specifically where the distal shaft of the ulna is reduced or fused (Howell, 1944; Polly, 2007). This increased pressure on the radius for support could explain why radioulna measurements were three of the five most preferred models (Supporting Information:Table S1). Most quadrupedal mammals, with the exception of primates (Demes et al., 1994; Fish et al., 2021; Raichlen et al., 2009; Schmitt & Lemelin, 2002), support more weight with their forelimbs than their hindlimbs because of a forwardly-placed center of mass. In particular, terrestrial runners, including cheetahs, camels, and dogs, tend to support mass on their forelimbs (Fish et al., 2021; Jayes & Alexander, 1978; Rollinson, 1981). Therefore, the radioulna might be demonstrating a stronger relationship to body size due to the forwardly-placed center of mass.

In addition to cursorial locomotion, large, heavy crania could further impact this forwardly-placed center of mass (Fish et al., 2021). The long neck of a giraffe is likely to also place increased pressure on the forelimbs compared to hindlimbs, and experimental data has shown that the center of mass is forwardly placed in giraffes (Basu et al., 2019; Henderson & Naish, 2010). Ruminant artiodactyls could be particularly susceptible to increased force on the forelimbs due to the weight of headgear, particularly in members of Bovidae and Cervidae. However, there is considerable variability in the presence or absence of headgear throughout Ruminantia (Davis et al., 2011; Janis & Theodor, 2014). Some species are sexually dimorphic, with only males having headgear (e.g,. greater kudu, elk), while headgear may also be present in both sexes of a species (e.g., reindeer, giraffes) or neither sex (e.g., musk deer; Brakora, 2012; Geist & Bayer, 1988; Packer, 1983). It is unclear what effect headgear has on the anterior body weight, or if headgear weight is taken into account when body masses are reported in the literature. Future work should examine the impact of headgear on artiodactyl weight and forwardly placed mass.

### 4.4 | Tarsal bone estimation

Tarsal bones have been used to estimate mammal locomotion and ecomorphology due to the crucial role they play in ankle and hindlimb mechanics, and because they are frequently preserved in the fossil record (Barr, 2018; Bassarova et al., 2009; Ginot et al., 2016; Polly, 2008; Tsubamoto, 2019; Yapuncich et al., 2015). Martinez and Sudre (1995) suggested that overall astragalus dimensions (length and width) were more useful predictors of mass in Paleogene artiodactyls than dental proxies in many cases. Using a diverse sample of mammals, Tsubamoto (2014) found that, among a variety of astragalar shapes, the transverse width of the trochlea of the astragalus, which articulates with the tibia, was the most reliable predictor. With a sample consisting mostly of carnivorans and primates and few artiodactyls, Tsubamoto (2019) found that the width of the calcaneus encompassing two surfaces that articulate with the astragalus was the best predictor of body mass.

Measurements from the calcaneus and astragalus were average predictors of body mass in ruminant artiodactyls compared to other models based on AIC score (Supporting Information: Table S1) with the exception of the calcaneus stepwise regression model, which was comparable to the humerus stepwise regression model and radioulna models when all models were compared. However, when either bone is found in isolation, multiple regression and individual regressions can perform with similar accuracy for each bone. The best model for the calcaneus used multiple measurements, but the height of the sustentacular facet was similarly preferred (C8, Table 3). The single measurement of the astragalar width at tarsus was the best model for predicting mass based on that bone. That individual measurements work well, but multiple are as preferred for the calcaneus, is especially important given the robustness of these bones and their high preservation potential in the fossil record, particularly the astragalus, which is a relatively dense, abundantly preserved bone that is resistant to hydraulic transport (Behrensmeyer, 1975; DeGusta & Vrba, 2003; Hussain et al., 1983; Tsubamoto, 2014).

The astragalus is especially diagnostic of ruminants, and of artiodactyls more generally, because of its double pulley morphology (Schaeffer, 1947; Thewissen & Madar, 1999). However, the application of astragalus measurements to predict mass in fossil ruminants does not come without concern. While the calcaneus has a recognizable growth plate on the distal end of the tuber, which indicates whether or not the individual is fully grown (Jogahara & Natori, 2013), the modern artiodactyl astragalus has no known observable growth plates. This is problematic because most studies exclusively sample adult or fully grown specimens to predict mass, and astragalus specimens with unidentifiable growth plates lead to uncertainty regarding maturity when sampling fossil specimens, unless they are associated with other remains. For the purposes of

identifying fully grown individuals, it may be more practical to use the calcaneus or long bone epiphyses because it is more likely that these regions will provide evidence of individual maturity.

### 4.5 | Using %PE and applications to fossils

Percent prediction error (%PE) is a commonly used metric to assess how a data point is over- or underpredicted using a particular regression (Smith, 1984; Van Valkenburgh, 1990). However, simply averaging the %PE of all data points in a sample can mask considerable variation in predictive accuracy among individuals. Table 4 shows the variation on average %PE at the family, subfamily, and tribe levels for the global most and least preferred models. The best model for predicting mass in this sample of ruminants (humerus stepwise multiple regression), shows a reasonable average %PE for Bovidae (−2.25), but members of the closely related tribes Bovini and Boselaphini have quite different averages (7.05 and 0.13, respectively). Two species in Bovini specifically show vastly different %PEs for the humerus stepwise model; *Bos sauveli* (kouprey) is underpredicted by 16.62%, and the tamaraw (*Bubalus mindorensis*) has a %PE of 0. Therefore, considerable variation may persist at lower taxonomic levels despite a reasonable average %PE for the total sample. The potential contrast in %PE among species and regressions should be considered when using regressions to predict mass for extinct or extant ruminants.

An important consideration for the results presented here are how to apply them to estimate the mass of fossil ruminants. Knowing which model(s) provide the best fit for a particular species (or alternative taxonomic level) can be useful for finding the most appropriate regressions to predict mass in a closely related fossil taxon (Supporting Information). I used two regressions to predict mass for *B. antiquus*, the preferred global regression and the Bovini-specific regression, which resulted in a range of masses from roughly 800.45–883 kg. Martin et al. (2018) used calcaneal measurements to predict the mass of several bison species and estimated *B. antiquus* to be 802 kg, which is more consistent with my *B. antiquus* estimates from the humerus stepwise multiple regression (best for all ruminants), though their estimate included an error of ±183 kg.

*Aletomeryx* was previously predicted by Scott (1983) and Scott (1990) to be 19–23.2 kg and 15–23 kg, respectively. The stepwise humerus regression predicts *Aletomeryx* as a reasonable 22.16 kg, and the stepwise radius regression predicts a similar value of 23.21 kg (Table 5). Finally, the pronghorn relative, *Cosoryx furcatus*, was predicted here using the stepwise humerus regression as 14.64 kg, but using the best model for Antilocapridae (tibia midshaft circumference), I estimated it to be 14.05 kg. All of my estimates were higher than that reported by Scott (1983; 7.6–11.8 kg). Regardless, estimations from the global preferred regression of humerus elements and the clade-level regression used for each fossil taxon generally agree with one another, suggesting that using %PE allows for flexibility in selecting the most appropriate regression model for a given fossil. This finding is important because it allows flexibility in what measurements can be used to predict mass based on available fossil remains despite potential differences in %PE among species within a regression. Even more crucial is the indication that, based on the preliminary evidence presented here, regressions at the family level can well predict the body size of extinct taxa with little to no extant representatives, as is the case for *Aletomeryx* and *C. furcatus*.

## 5 | CONCLUSION

Estimating body mass is crucial for understanding the ecology of fossil mammals, particularly in ruminants, which have a unique relationship between body mass and ecology. Here, I assessed the best predictors of body mass in a sample of extant ruminants using individual measurements and groups of measurements from whole postcranial bones and concentrations at long bone ends. I found that, in many cases, using measurement subsets of a bone determined by stepwise regression yielded the best predictors of body mass for that element, particularly the regression involving humerus proximal and distal widths, which represented the global optimal model for predicting mass among ruminants as a whole. However, several bivariate and stepwise multiple regression models from the radioulna were considered equally optimal according to AIC scores, as well as the stepwise calcaneus model. Widths in general seem to be reliable indicators of mass throughout the postcranial skeleton, which suggests that changes to mass in extreme cases are likely reflected in transverse stresses of long bones. Finally, differences in %PE at the subclade level can be used as an informative guide for choosing a model with which to predict the body mass of fossil ruminants, providing a new framework and novel tools with which to study body mass evolution in ruminant artiodactyls and mammals broadly.

### AUTHOR CONTRIBUTIONS

**Alexa N. Wimberly**: Conceptualization; investigation; writing—original draft; methodology; validation; visualization; writing—review and editing; formal analysis; project administration; data curation; supervision; resources; funding acquisition; software.

### ACKNOWLEDGMENTS

I am grateful for the funding and support from the Smithsonian Institution Predoctoral Fellowship program as well as the Field Museum Women in Science Graduate Student Fellowship. I thank Juan P. Zurano, Daniel O. Mesquita, and Gabriel C. Costa for sharing with me the nexus file and full mitochondrial genome alignment for my phylogenetic analyses. Graham Slater provided feedback throughout this project and the writing process. I also thank one anonymous reviewer for their helpful comments which improved this manuscript. I am grateful to museum staff and collections managers Adam Ferguson at the Field Museum of Natural History, Melissa Hawkins, Darrin Lunde, and John Ososky at the Smithsonian National Museum of Natural History, and Jin Meng and Judy Galkin at the American Museum of Natural History.

## CONFLICT OF INTEREST STATEMENT

The author declares no conflict of interest.

## DATA AVAILABILITY STATEMENT

R scripts and data files have been deposited on Data Dryad. (https://doi.org/10.5061/dryad.8sf7m0ctf).

## ORCID

*Alexa N. Wimberly* http://orcid.org/0000-0002-2601-6540

## PEER REVIEW

The peer review history for this article is available at https://www.webofscience.com/api/gateway/wos/peer-review/10.1002/jmor.21636.

## REFERENCES

Alexander, R. M., Jayes, A. S., Maloiy, G. M. O., & Wathuta, E. M. (1979). Allometry of the limb bones of mammals from shrews (*Sorex*) to elephant (*Loxodonta*). *Journal of Zoology*, *189*, 305–314.

Alroy, J. (1998). Cope's rule and the dynamics of body mass evolution in North American fossil mammals. *Science*, *280*, 731–734.

Anderson, J. F., Hall-Martin, A., & Russell, D. A. (1985). Long-bone circumference and weight in mammals, birds and dinosaurs. *Journal of Zoology*, *207*, 53–61.

Andersson, K. (2004). Predicting carnivoran body mass from a weight-bearing joint. *Journal of Zoology*, *262*, 161–172.

Anyonge, W. (1993). Body mass in large extant and extinct carnivores. *Journal of Zoology*, *231*, 339–350.

Bakker, R. T. (1983). The deer flees, the wolf pursues: Incongruencies in predatorprey coevolution. In D. J. Futuyma, & M. Slatkin (Eds.), *Coevolution* (pp. 350–382). Sinauer.

Barr, A. W. (2018). The morphology of the bovid calcaneus: Function, phylogenetic signal, and allometric scaling. *Journal of Mammalian Evolution*, *27*, 111–121.

Bassarova, M., Janis, C. M., & Archer, M. (2009). The calcaneum—on the heels of marsupial locomotion. *Journal of Mammalian Evolution*, *16*, 1–23.

Basu, C., Falkingham, P. L., & Hutchinson, J. R. (2016). The extinct, giant giraffid *Sivatherium giganteum*: Skeletal reconstruction and body mass estimation. *Biology Letters*, *12*, 20150940.

Basu, C., Wilson, A. M., & Hutchinson, J. R. (2019). The locomotor kinematics and ground reaction forces of walking giraffes. *The Journal of Experimental Biology*, *222*, jeb159277.

Behrensmeyer, A. K. (1975). The taphonomy and paleoecology of Plio-Pleistocene vertebrate assemblages east of Lake Rudolf, Kenya. *Bulletin of the Museum of Comparative Zoology*, *146*, 473–578.

Bertram, J. E. A., & Biewener, A. A. (1990). Differential scaling of the long bones in the terrestrial Carnivora and other mammals. *Journal of Morphology*, *204*, 157–169.

Bertram, J. E. A., & Biewener, A. A. (1992). Allometry and curvature in the long bones of quadrupedal mammals. *Journal of Zoology*, *226*, 455–467.

Biewener, A. A. (1983). Allometry of quadrupedal locomotion: The scaling of duty factor, bone curvature and limb orientation to body size. *Journal of Experimental Biology*, *105*, 147–171.

Biewener, A. A. (1989). Scaling body support in mammals: Limb posture and muscle mechanics. *Science*, *245*, 45–48.

Biewener, A. A. (1990). Biomechanics of mammalian terrestrial locomotion. *Science*, *250*, 1097–1103.

Biknevicius, A. R. (1993). Biomechanical scaling of limb bones and differential limb use in caviomorph rodents. *Journal of Mammalogy*, *74*, 95–107.

Biknevicius, A. R. (1999). Body mass estimation in armoured mammals: Cautions and encouragements for the use of parameters from the appendicular skeleton. *Journal of Zoology*, *248*, 179–187.

Brakora, K. A. (2012). *Evolution and development of sexual dimorphism in African antelope*. University of California.

Calder, W. A. (1996). *Size, function, and life history*. Harvard University Press.

Campione, N. E., & Evans, D. C. (2012). A universal scaling relationship between body mass and proximal limb bone dimensions in quadrupedal terrestrial tetrapods. *BMC Biology*, *10*, 60.

Carrano, M. T. (2001). Implications of limb bone scaling, curvature and eccentricity in mammals and non-avian dinosaurs. *Journal of Zoology*, *254*, 41–55.

Christiansen, P. (1999). Scaling of the limb long bones to body mass in terrestrial mammals. *Journal of Morphology*, *239*, 167–190.

Damuth, J., & MacFadden, B. J. (1990). *Body size in mammalian paleobiology: Estimation and biological implications*. Cambridge University Press.

Davis, E. B., Brakora, K. A., & Lee, A. H. (2011). Evolution of ruminant headgear: A review. *Proceedings of the Royal Society B: Biological Sciences*, *278*, 2857–2865.

DeGusta, D., & Vrba, E. (2003). A method for inferring paleohabitats from the functional morphology of bovid astragali. *Journal of Archaeological Science*, *30*, 1009–1022.

Demes, B., Larson, S. G., Stern, Jr. J. T., Jungers, W. L., Biknevicius, A. R., & Schmitt, D. (1994). The kinetics of primate quadrupedalism: "Hindlimb drive" reconsidered. *Journal of Human Evolution*, *26*, 353–374.

Egi, N. (2001). Body mass estimates in extinct mammals from limb bone dimensions: The case of North American hyaenodontids. *Palaeontology*, *44*, 497–528.

Eisenberg, J. (1981). *The mammalian radiations: An analysis of trends in evolution, adaptation, and behavior*. University of Chicago Press.

Figueirido, B., Pérez-Claros, J. A., Hunt, R. M., & Palmqvist, P. (2011). Body mass estimation in amphicyonid carnivoran mammals: A multiple regression approach from the skull and skeleton. *Acta Palaeontologica Polonica*, *56*, 225–246.

Finarelli, J. A., & Flynn, J. J. (2006). Ancestral state reconstruction of body size in the Caniformia (Carnivora, Mammalia): The effects of incorporating data from the fossil record. *Systematic Biology*, *55*, 301–313.

Fish, F. E., Sheehan, M. J., Adams, D. S., Tennett, K. A., & Gough, W. T. (2021). A 60: 40 split: Differential mass support in dogs. *The Anatomical Record*, *304*, 78–89.

Gambaryan, P. P. (1974). *How mammals run: Anatomical adaptations*. Wiley.

Garland, T., & Janis, C. M. (1993). Does metatarsal/femur ratio predict maximal running speed in cursorial mammals? *Journal of Zoology*, *229*, 133–151.

Geist, V., & Bayer, M. (1988). Sexual dimorphism in the Cervidae and its relation to habitat. *Journal of Zoology*, *214*, 45–53.

Gingerich, P. D. (1990). Prediction of body mass in mammalian species from long bone lengths and diameters. *Contributions from the Museum of Paleontology, The University of Michigan*, *28*, 79–92.

Gingerich, P. D., Smith, B. H., & Rosenberg, K. (1982). Allometric scaling in the dentition of primates and prediction of body weight from tooth size in fossils. *American Journal of Physical Anthropology*, *58*, 81–100.

Ginot, S., Hautier, L., Marivaux, L., & Vianey-Liaud, M. (2016). Ecomorphological analysis of the astragalo-calcaneal complex in rodents and inferences of locomotor behaviours in extinct rodent species. *PeerJ*, *4*, e2393.

Henderson, D. M., & Naish, D. (2010). Predicting the buoyancy, equilibrium and potential swimming ability of giraffes by computational analysis. *Journal of Theoretical Biology*, *265*, 151–159.

Howell, A. B. (1944). *Speed in animals, their specialization for running and leaping*. University of Chicago Press.

Hussain, S. T., Sondaar, P., Shah, S., Thewissen, J., Cousin, E., & Spoor, C. (1983). Fossil mammal bones of Pakistan—a field atlas. -Part I: The artiodactyl astragalus. *Memoirs of the Geological Survey of Pakistan*, *14*, 1–15.

Janis, C. M. (1990). Correlation of cranial and dental variables with dietary preferences in mammals: A comparison of macropodoids and ungulates. In J. D. Damuth, & B. J. MacFadden (Eds.), *Body size in mammalian paleobiology: Estimation and biological implications* (pp. 255–299). Cambridge University Press.

Janis, C. M., & Scott, K. M. (1987). The interrelationships of higher ruminant families: With special emphasis on the members of the Cervoidea. *American Museum Novitates*, *2*, 893.

Janis, C. M., & Theodor, J. M. (2014). Cranial and postcranial morphological data in ruminant phylogenetics. *Zitteliana B*, *32*, 15–31.

Janis, C. M., & Wilhelm, P. B. (1993). Were there mammalian pursuit predators in the tertiary? Dances with wolf avatars. *Journal of Mammalian Evolution*, *1*, 103–125.

Jayes, A. S., & Alexander, R. M. (1978). Mechanics of locomotion of dogs (*Canis familiaris*) and sheep (*Ovis aries*). *Journal of Zoology*, *185*, 289–308.

Jogahara, Y. O., & Natori, M. (2013). Talar maturity determined by epiphyseal closure of the calcaneus. *Folia Primatologica*, *84*, 11–17.

Kappelman, J., Plummer, T., Bishop, L., Duncan, A., & Appleton, S. (1997). Bovids as indicators of Plio-Pleistocene paleoenvironments in East Africa. *Journal of Human Evolution*, *32*, 229–256.

Kubo, T., Sakamoto, M., Meade, A., & Venditti, C. (2019). Transitions between foot postures are associated with elevated rates of body size evolution in mammals. *Proceedings of the National Academy of Sciences*, *116*, 2618–2623.

Legendre, S. (1986). Analysis of mammalian communities from the late Eocene and Oligocene of southern France. *Palaeovertebrata*, *16*, 191–212.

Legendre, S., & Roth, C. (1988). Correlation of carnassial tooth size and body weight in recent carnivores (Mammalia). *Historical Biology*, *1*, 85–98.

Lindstedt, S. L., Miller, B. J., & Buskirk, S. W. (1986). Home range, time, and body size in mammals. *Ecology*, *67*, 413–418.

Martin, J. M., Mead, J. I., & Barboza, P. S. (2018). Bison body size and climate change. *Ecology and Evolution*, *8*, 4564–4574.

Martinez, J.-N., & Sudre, J. (1995). The astragalus of Paleogene artiodactyls: Comparative morphology, variability and prediction of body mass. *Lethaia*, *28*, 197–209.

McNab, B. K. (1988). Complications inherent in scaling the basal rate of metabolism in mammals. *The Quarterly Review of Biology*, *63*, 25–54.

Mendoza, M., Janis, C. M., & Palmqvist, P. (2006). Estimating the body mass of extinct ungulates: A study on the use of multiple regression. *Journal of Zoology*, *270*, 90–101.

Millien, V., & Bovy, H. (2010). When teeth and bones disagree: Body mass estimation of a giant extinct rodent. *Journal of Mammalogy*, *91*, 11–18.

Packer, C. (1983). Sexual dimorphism: The horns of African antelopes. *Science*, *221*, 1191–1193.

Peters, R. H. (1986). *The ecological implications of body size*. Cambridge University Press.

Pineda-Munoz, S., Evans, A. R., & Alroy, J. (2016). The relationship between diet and body mass in terrestrial mammals. *Paleobiology*, *42*, 659–669.

Pinheiro, J., Bates, D., DebRoy, S., Sarkar, D., Heisterkamp, S., Van Willigen, B., & Maintainer, R., 2017. Package 'nlme'. R package version 3 3:274.

Polly, P. D. (2007). Limbs in mammalian evolution. In B. Hall (Ed.), *Fins into limbs: Evolution, development and transformation* (pp. 245–268). University of Chicago Press Chicago.

Polly, P. D. (2008). Adaptive zones and the pinniped ankle: A three-dimensional quantitative analysis of carnivoran tarsal evolution. In E. J. Sargis, & M. Dagosto (Eds.), *Mammalian evolutionary morphology* (pp. 167–196). Springer.

Price, S. A., & Hopkins, S. S. B. (2015). The macroevolutionary relationship between diet and body mass across mammals. *Biological Journal of the Linnean Society*, *115*, 173–184.

Prothero, D. R., & Liter, M. R. (2008). Systematics of the dromomerycines and aletomerycines (Artiodactyla: Palaeomerycidae) from the Miocene and Pliocene of North America. *New Mexico Museum of Natural History and Science Bulletin*, *44*, 273–298.

Raichlen, D. A., Pontzer, H., Shapiro, L. J., & Sockol, M. D. (2009). Understanding hind limb weight support in chimpanzees with implications for the evolution of primate locomotion. *American Journal of Physical Anthropology*, *138*, 395–402.

Reilly, S. M., McElroy, E. J., & Biknevicius, A. R. (2007). Posture, gait and the ecological relevance of locomotor costs and energy-saving mechanisms in tetrapods. *Zoology*, *110*, 271–289.

Revell, L. J. (2012). Phytools: An R package for phylogenetic comparative biology (and other things): Phytools: R package. *Methods in Ecology and Evolution*, *3*, 217–223.

Reynolds, P. S. (2002). How big is a giant? The importance of method in estimating body size of extinct mammals. *Journal of Mammalogy*, *83*, 321–332.

Ripley, B., Venables, B., Bates, D. M., Hornik, K., Gebhardt, A., Firth, D., & Ripley, M. B. (2013). Package 'mass'. *Cran r*, *538*, 113–120.

Rollinson, J. (1981). Comparative aspects of primate locomotion, with special reference to arboreal cercopithecines. in Symposia of the Zoological Society of London, vol. 48, 377–427.

Rothier, P. S., Fabre, A.-C., Clavel, J., Benson, R. B., & Herrel, A. (2023). Mammalian forelimb evolution is driven by uneven proximal-to-distal morphological diversity. *eLife*, *12*, e81492.

Ruff, C. (1988). Hindlimb articular surface allometry in Hominoidea and Macaca, with comparisons to diaphyseal scaling. *Journal of Human Evolution*, *17*, 687–714.

Ruff, C. (1990). Body mass and hindlimb bone cross-sectional and articular dimensions in anthropoid primates. In J. D. Damuth, & B. J. MacFadden (Eds.), *Body size in mammalian paleobiology: Estimation and biological implications*, (119–149). Cambridge University Press.

Ruff, C. B. (2003). Long bone articular and diaphyseal structure in old world monkeys and apes. ii: Estimation of body mass. *American Journal of Physical Anthropology*, *120*, 16–37.

Sánchez-Villagra, M. R., Aguilera, O., & Horovitz, I. (2003). The anatomy of the world's largest extinct rodent. *Science*, *301*, 1708–1710.

Schaeffer, B. (1947). Notes on the origin and function of the artiodactyl tarsus. *American Museum Novitates*, *1356*, 1–24.

Schmidt-Nielsen, K. (1984). *Scaling: Why is animal size so important?* Cambridge University Press.

Schmitt, D., & Lemelin, P. (2002). Origins of primate locomotion: Gait mechanics of the woolly opossum. *American Journal of Physical Anthropology*, *118*, 231–238.

Scott, K. M. (1983). Prediction of body weight of fossil Artiodactyla. *Zoological Journal of the Linnean Society*, *77*, 199–215.

Scott, K. M. (1985). Allometric trends and locomotor adaptations in the Bovidae. Bulletin of the American Museum of Natural History (USA).

Scott, K. M. (1990). Postcranial dimensions of ungulates as predictors of body mass. In J. D. Damuth, & B. J. MacFadden (Eds.), *Body size in mammalian paleobiology: Estimation and biological implications* (pp. 301–335). Cambridge University Press.

Smith, J. M., & Savage, R. J. G. (1956). Some locomotory adaptations in mammals. *Journal of the Linnean Society of London, Zoology*, *42*, 603–622.

Smith, R. J. (1984). Allometric scaling in comparative biology: Problems of concept and method. *American Journal of Physiology-Regulatory, Integrative and Comparative Physiology*, *246*, R152–R160.

Swihart, R. K., Slade, N. A., & Bergstrom, B. J. (1988). Relating body size to the rate of home range use in mammals. *Ecology*, *69*, 393–399.

Thewissen, J. G. M., & Madar, S. I. (1999). Ankle morphology of the earliest cetaceans and its implications for the phylogenetic relations among ungulates. *Systematic Biology*, *48*, 21–30.

Tsubamoto, T. (2014). Estimating body mass from the astragalus in mammals. *Acta Palaeontologica Polonica*, *59*, 259–265.

Tsubamoto, T. (2019). Relationship between the calcaneal size and body mass in primates and land mammals. *Anthropological Science*, *127*, 73–80.

Tucker, M. A., Ord, T. J., & Rogers, T. L. (2014). Evolutionary predictors of mammalian home range size: Body mass, diet and the environment. *Global Ecology and Biogeography*, *23*, 1105–1114.

Van Valkenburgh, B. (1990). Skeletal and dental predictors of body mass in carnivores. In J. D. Damuth, & B. J. MacFadden (Eds.), *Body size in mammalian paleobiology: Estimation and biological implications* (pp. 181–205). Cambridge University Press.

Yapuncich, G. S., Gladman, J. T., & Boyer, D. M. (2015). Predicting euarchontan body mass: A comparison of tarsal and dental variables. *American Journal of Physical Anthropology*, *157*, 472–506.

Young, N. M. (2013). Macroevolutionary diversity of amniote limb proportions predicted by developmental interactions. *Journal of Experimental Zoology Part B: Molecular and Developmental Evolution*, *320*(7), 420–437.

Zurano, J. P., Magalhães, F. M., Asato, A. E., Silva, G., Bidau, C. J., Mesquita, D. O., and Costa, G. C. (2019). Cetartiodactyla: Updating a time-calibrated molecular phylogeny. *Molecular Phylogenetics and Evolution 133*:256–262.

## SUPPORTING INFORMATION

Additional supporting information can be found online in the Supporting Information section at the end of this article.

**How to cite this article:** Wimberly, A. N. (2023). Predicting body mass in Ruminantia using postcranial measurements. *Journal of Morphology*, *284*, e21636. https://doi.org/10.1002/jmor.21636